Journal of Solid State Chemistry **153,** 270–274 (2000)
doi:10.1006/jssc.2000.8754, available online at http://www.idealibrary.com on IDEAL®

Evidence of Anionic Disorder in Fluoride Borate $Eu_3(BO_3)_2F_3$ from Eu^{3+} Luminescence: Comparison with Fluoride Carbonate $Ba_2Eu(CO_3)_2F_3$

Elisabeth Antic-Fidancev,*,[1] Gwenaël Corbel,† Nicolas Mercier,‡ and Marc Leblanc†

*Laboratoire de Chimie Appliquée de l'Etat Solide, CNRS, UMR-7574, ENSCP, 11 Rue Pierre et Marie Curie, 75231 Paris Cedex 05, France; †Laboratoire des Fluorures UPRES-A 6010, Faculté des Sciences, Avenue Olivier Messiaen, 72085 Le Mans Cedex 09, France; and ‡Laboratoire IMMO, UMR-6501, Faculté des Sciences, 2 Boulevard Lavoisier, 49045 Angers, France

Received February 24, 2000; in revised form April 12, 2000; accepted April 20, 2000; published online July 18, 2000

The optical behavior of europium fluoride borate $Eu_3(BO_3)_2F_3$ and barium fluoride carbonates $Ba_2Eu(CO_3)_2F_3$ is investigated with Eu^{3+} as a local structural probe. Tentative correlation between the optical and structural data are discussed. Unexpected broad emission lines are observed for Eu^{3+} in fluoride borate and the separation of two crystallographic sites, predicted from the structure determination, is impossible. It is assumed that deviation from the ideal stoichiometry $Eu_3(BO_3)_2F_3$ occurs and is due to the substitution $BO_3^{3-} \leftrightarrow 3F^-$, leading to the formulation $Eu_3(BO_3)_{2+x}F_{3-3x}$. Crystal field analysis is performed on the ^7F_J basis of the $4f^6$ configuration of Eu^{3+}. The crystal field parameters (*cfp*) and crystal field strength parameter N_V are similar for both compounds though slightly larger for $Eu_3(BO_3)_2F_3$ This difference is especially significant for two rank (*cfp*), indicative of a larger electrostatic field in $Eu_3(BO_3)_2F_3$.

Key Words: **fluoride borate; fluoride carbonate; europium luminescence; crystal field analysis.**

INTRODUCTION

Numerous fluoride carbonates, eventually isostructural with natural minerals, can be synthesized under hydrothermal conditions and several new rare earth or transition metal compounds were recently evidenced (1). In contrast, the hydrothermal growth of fluoride borates is difficult: boracites $M_3B_7O_{13}F$ are obtained only for $M^{2+} = 3d$ transition metals (2). Rare earth fluoride borates were unknown until the solid state synthesis of $RE_3(BO_3)_2F_3$ phases for RE = Sm, Eu, and Gd (3). The structure of $RE_3(BO_3)_2F_3$ is built up from the stacking of REX_9 polyhedra (X = O and F), very similar to the REX_9 or BaX_9 polyhedra found in $Ba_2RE(CO_3)_2F_3$ (4). Both compounds present the same cation/anion ratio and this analogy can be expressed by the following hypothetical exchange: $3RE^{3+} + 2BO_3^{3-} \leftrightarrow 2Ba^{2+} + RE^{3+} + 2CO_3^{2-}$.

We present here the luminescence study of europium Eu^{3+} in the fluoride borates $Eu_3(BO_3)_2F_3$ or $Gd_3(BO_3)_2F_3$: Eu^{3+} and in the fluoride carbonate $Ba_2Eu(CO_3)_2F_3$.

CRYSTAL STRUCTURE DESCRIPTION

In both title compounds, rare earth or barium cations adopt a ninefold coordination with a low-site symmetry: C_2 for Eu^{3+} and C_1 for Ba^{2+} in $Ba_2Eu(CO_3)_2F_3$ and C_2 for Eu(1) and C_1 for Eu(2) in $Eu_3(BO_3)_2F_3$. The structure is performed on $Gd_3(BO_3)_2F_3$ as well as on $Ba_2Gd(CO_3)_2F_3$ crystals and the polyhedral arrangements are shown in Fig. 1 (3, 4). The nature of the coordination anions differs in both phases: EuO_6F_3 and BaO_5F_4 in $Ba_2Eu(CO_3)_2F_3$, $Eu(1)O_4F_5$, and $Eu(2)O_7F_2$ in $Eu_3(BO_3)_2F_3$. However, it is remarkable that very similar trimeric units, $Ba_2EuO_{12}F_9$ and $Eu_3O_{14}F_9$, are found in $Ba_2Eu(CO_3)_2F_3$ and $Eu_3(BO_3)_2F_3$, respectively. These units, centered on a twofold axis, result from the connection of two polyhedra to the central polyhedron by triangular O_2F faces in $Ba_2Eu(CO_3)_2F_3$ and by oxygen edges in $Eu_3(BO_3)_2F_3$. The resulting $Ba_2EuO_{12}F_9$ or $Eu_3O_{14}F_9$ trimers, linked by borate groups and connected to each other, build up the three-dimensional (3D) networks. They form infinite "herring bone" chains in $Ba_2Eu(CO_3)_2F_3$, whereas they are parallel in $Eu_3(BO_3)_2F_3$.

EXPERIMENTAL DETAILS

The luminescence of powder samples of $Ba_2Eu(CO_3)_2F_3$, $Eu_3(BO_3)_2F_3$, and $Gd_3(BO_3)_2F_3$: Eu^{3+} was measured at 77 K by using the blue line ($\lambda_{exc} = 457.9$ nm) of a 5-W Spectra Physics argon ion laser. Selective excitation of the respective $^5D_0 \rightarrow {}^7F_0$ transitions was performed with a rhodamine 6G dye laser pumped by the argon ion laser.

[1]To whom correspondence should be addressed. E-mail: antic@ext.jussieu.fr.

0022-4596/00 $35.00

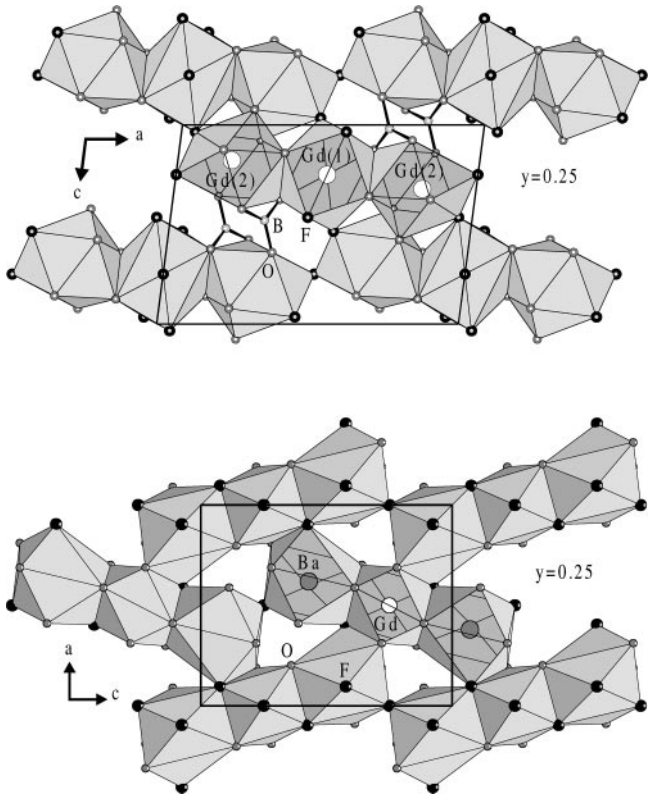

FIG. 1. Polyhedral arrangement in $Gd_3(BO_3)_2F_3$ (up) and in $Ba_2Gd(CO_3)_2F_3$ (down).

Fluorescence emission was detected through a 1-m Jarrell Ash monochromator equipped with a Hamamatsu R374 photomultiplier.

It must be noted that the synthesis of pure compounds is difficult and impurity phases are detected; $Ba_2Eu(CO_3)_2F_3$, $Eu_3(BO_3)_2F_3$, and $Gd_3(BO_3)_2F_3$:Eu^{3+} are contaminated with small amounts of $BaEu(CO_3)_2F$ (huangoite), $EuBO_3$ (triclinic), and $GdBO_3$ (vaterite), respectively.

OPTICAL DATA

The emission spectrum of raw $Ba_2Eu(CO_3)_2F_3$, excited by the 457.9-nm wavelength, consists of sharp and intense peaks associated with the $^5D_0 \rightarrow {}^7F_{0-4}$ transitions. One line and four lines are observed respectively for the $^5D_0 \rightarrow {}^7F_0$ and for the $^5D_0 \rightarrow {}^7F_1$ transitions (Fig. 2). Selective excitation of the unique $^5D_0 \rightarrow {}^7F_0$ transition at $\lambda = 579.75$ nm gives three $^5D_0 \rightarrow {}^7F_1$ lines, attributed to $Ba_2Eu(CO_3)_2F_3$. The extra line at $\lambda = 589.0$ nm corresponds to the intense $^5D_0 \rightarrow {}^7F_1$ line of huangoite $BaEu(CO_3)_2F$, which presents a very weak $^5D_0 \rightarrow {}^7F_0$ transition at $\lambda = 579.05$ nm. The selective excitation of the fluoride carbonate mixture at this wavelength confirms unambiguously the presence of $BaEu(CO_3)_2F$ (Fig. 2).

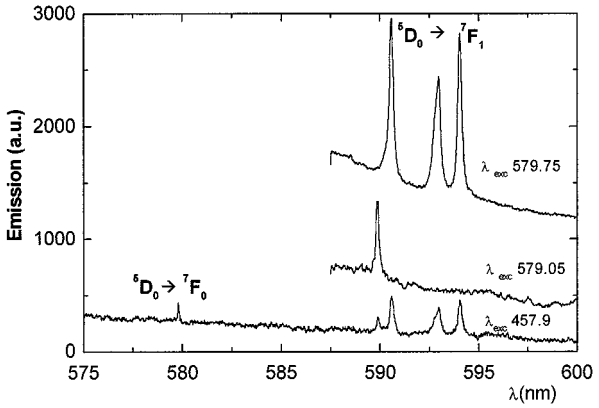

FIG. 2. Parts of emission spectra at 77 K under argon ion laser (bottom) and dye excitation of Eu^{3+} in $Ba_2Eu(CO_3)_2F_3$ ($\lambda_{exc} = 579.75$ nm) and $BaEu(CO_3)_2F$ ($\lambda_{exc} = 579.05$ nm).

In contrast, the emission spectra of raw $Eu_3(BO_3)_2F_3$ or $Gd_3(BO_3)_2F_3$:Eu^{3+} consist of weak and broad lines associated with very few small peaks attributed to impurity phases. Selective excitation of the $^5D_0 \rightarrow {}^7F_0$ transitions situated at $\lambda = 579.59$ nm and $\lambda = 580.49$ nm for Eu^{3+} in raw $Eu_3(BO_3)_2F_3$ (Fig. 3) gives respectively three broad lines and five sharp $^5D_0 \rightarrow {}^7F_1$ lines. The broad lines belong to the title compound, $Eu_3(BO_3)_2F_3$, and the five sharp lines are associated with the presence of the impurity L-$EuBO_3$ (triclinic) in which two local environments are found for the rare earth ions (5). The full width at half maximum (FWHM) of the $^5D_0 \rightarrow {}^7F_0$ transition in $Eu_3(BO_3)_2F_3$ is approximately 90 cm^{-1}, not far from the value given for the europium in borosilicate glass (6). The emission spectrum of Eu^{3+} in raw $Gd_3(BO_3)_2F_3$:Eu^{3+} (Fig. 4) is different from

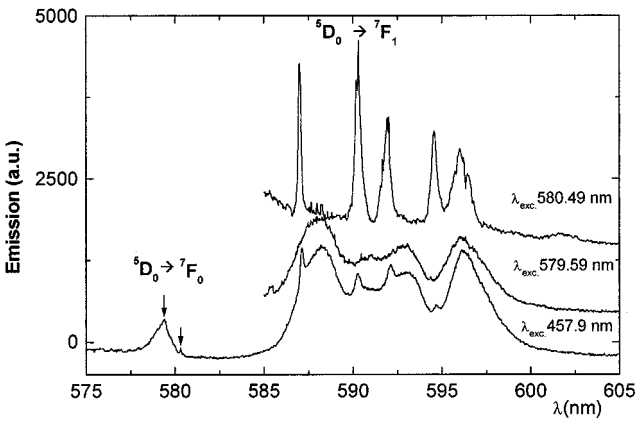

FIG. 3. Parts of emission spectra at 77 K under argon ion laser (bottom) and dye excitation of Eu^{3+} in $Eu_3(BO_3)_2F_3$ ($\lambda_{exc} = 579.59$ nm) and *L*-$EuBO_3$ ($\lambda_{exc} = 580.49$ nm).

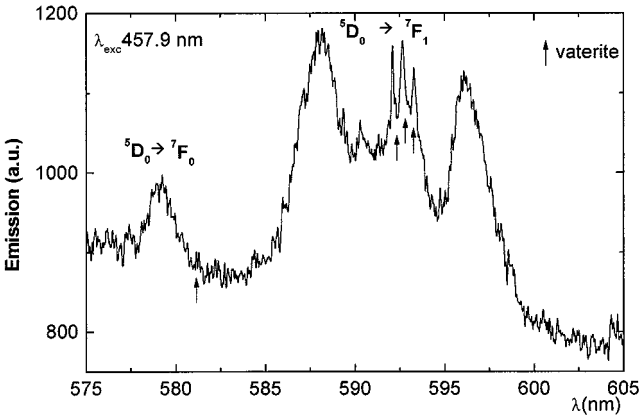

FIG. 4. Part of the emission spectra of Eu^{3+} in $Gd_3(BO_3)_2F_3$ under argon ion laser excitation at 77 K (arrows show the impurity phase).

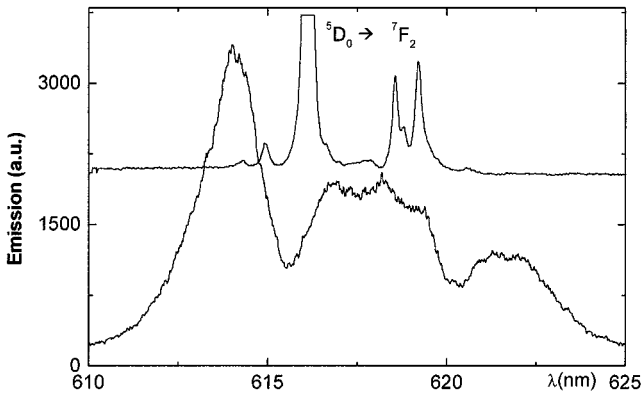

FIG. 6. Emission spectra at 77 K of Eu^{3+} in $Ba_2Eu(CO_3)_2F_3$ ($\lambda_{exc} = 579.75$ nm) and $Eu_3(BO_3)_2F_3$ ($\lambda_{exc} = 579.59$ nm) in the range of $^5D_0 \rightarrow {}^7F_2$ transitions.

that of $Eu_3(BO_3)_2F_3$. One broad $^5D_0 \rightarrow {}^7F_0$ band and three broad lines for the $^5D_0 \rightarrow {}^7F_1$ transitions are attributed to $Gd_3(BO_3)_2F_3$:Eu^{3+}. Thus, the spectra of pure $Eu_3(BO_3)_2F_3$ and $Gd_3(BO_3)_2F_3$:Eu^{3+} are very similar. Only three spurious $^5D_0 \rightarrow {}^7F_1$ sharp lines are observed in raw $Gd_3(BO_3)_2F_3$:Eu^{3+}; they correspond to the well-known orthoborate with the vaterite structure (7–10).

The comparison of the emission spectra, presented in Figs. 5 and 6, does not indicate any similarity between $Ba_2Eu(CO_3)_2F_3$ and $Eu_3(BO_3)_2F_3$ in relation to the presence of trimeric units, $Ba_2EuO_{12}F_9$ and $Eu_3O_{14}F_9$, respectively; this is especially obvious from the $^5D_0 \rightarrow {}^7F_2$ transitions. This result is at variance from our study on $BaEu(CO_3)_2F$ and $Na_3La_2(CO_3)_4F$:Eu^{3+} (11); in both structures, 10-fold coordinated REO_9F polyhedra generate almost matching emission spectra with small differences in the crystal field strength parameters.

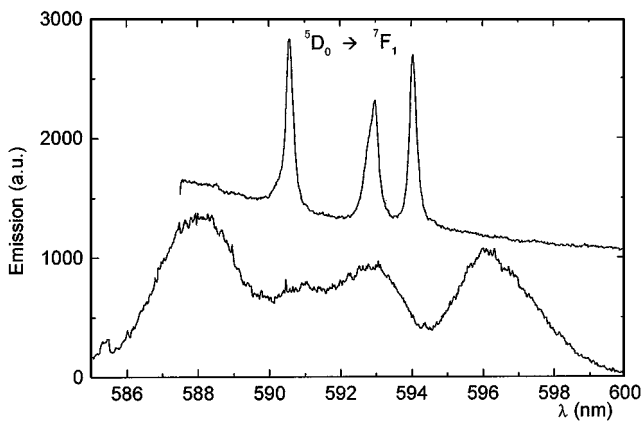

FIG. 5. Emission spectra at 77 K of Eu^{3+} in $Ba_2Eu(CO_3)_2F_3$ ($\lambda_{exc} = 579.75$ nm) and $Eu_3(BO_3)_2F_3$ ($\lambda_{exc} = 579.59$ nm) in the range of $^5D_0 \rightarrow {}^7F_1$ transitions.

CRYSTAL FIELD SIMULATION AND DISCUSSION

No selection rule for the electronic transitions observed in the optical spectra exists for rare earth ions at low-point symmetry sites; the degeneracy of every J level is completely lifted, giving rise respectively to $(2J + 1)$ crystal field levels. In addition, for C_n or C_{nv} symmetry only, the $^5D_0 \rightarrow {}^7F_0$ transition, which is totally forbidden at first order, becomes observable. The presence of this transition, as well as the exact number of Stark components observed for J-levels, confirms the low symmetry of the site occupied by Eu^{3+} ions in both studied compounds. In $Ba_2Eu(CO_3)_2F_3$ or $Eu_3(BO_3)_2F_3$, and also in doped $Gd_3(BO_3)_2F_3$:Eu^{3+} despite the low concentration of Eu^{3+}, a multiphonon deexcitation process quenches the emission from higher ^5D_J ($J = 1, 2$) levels. Thus, every emission line observed for Eu^{3+} originates from the $^5D_0$ level to the ground ^7F_J multiplets.

The energy levels assigned to $^7F_{0-4}$ manifolds (Tables 1 and 3), for $Eu_3(BO_3)_2F_3$ and $Ba_2Eu(CO_3)_2F_3$, respectively, were fitted by diagonalization of the crystal field parameter Hamiltonians through a refining procedure that minimizes the root mean square (r.m.s.) deviation of the calculated values (12). In the case of $Eu_3(BO_3)_2F_3$, the energy level simulation was completed for one average site. The obtained phenomenological crystal field parameters are collected in Tables 2 and 4 for $Eu_3(BO_3)_2F_3$ and $Ba_2Eu(CO_3)_2F_3$, respectively. It is worthwhile to notice that the resulting crystal field strength parameters, N_v, are mostly alike (13).

The crystal field parameters B_q^k are significant for neighbor participation in the crystal field of Eu^{3+}. The $k = 4$, 6 parameters are correlated with the crystal field which is induced by the nearest ligands. The $k = 2$ parameters, because of their importance in the point charge electrostatic field, give the contribution from next and further nearest

TABLE 1
Experimental and Calculated Energy Levels of Eu^{3+} in $Eu_3(BO_3)_2F_3$

$^{2S+1}L_J$ level	E_{exp} (cm^{-1})	E_{calc} (cm^{-1})	$^{2S+1}L_J$ level	E_{exp} (cm^{-1})	E_{calc} (cm^{-1})
$^7F_0$	0	0	$^7F_4$	2707	2708
				2723	2729
$^7F_1$	258	253		2821	2815
	394	392		2857	2865
	484	490		2881	2890
				2946	2938
$^7F_2$	975	970		2971	2966
	1047	1061		3045	3037
	1083	1075		3084	3090
	1108	1108			
	1169	1168	$^5D_0$	17253	
$^7F_3$	1847	1843			
	—	1862			
	1884	1881			
	1898	1898			
	—	1903			
	1984	1974			
	1984	1995			

TABLE 3
Experimental and Calculated Energy Levels of Eu^{3+} in $Ba_2Eu(CO_3)_2F_3$

$^{2S+1}L_J$ level	E_{exp} (cm^{-1})	E_{calc} (cm^{-1})	$^{2S+1}L_J$ level	E_{exp} (cm^{-1})	E_{calc} (cm^{-1})
$^7F_0$	0	0	$^7F_4$	2720	2720
				2742	2742
$^7F_1$	315	313		2775	2773
	384	381		2869	2860
	414	418		2886	2890
				2922	2921
$^7F_2$	967	969		2941	2934
	983	983		2974	2965
	1016	1024		3072	3075
	1078	1073			
	1095	1089	$^5D_0$	17245	
$^7F_3$	1901	1910			
	—	1954			
	—	1955			
	1966	1963			
	—	1993			
	—	2017			
	—	2023			

neighbors. They are associated with the $^7F_1$ multiplet splitting, which is small for $Ba_2Eu(CO_3)_2F_3$ in comparison to that for $Eu_3(BO_3)_2F_3$ (Fig. 5); the electrostatic field is larger in $Eu_3(BO_3)_2F_3$ than in $Ba_2Eu(CO_3)_2F_3$.

It was already noted that sharp and intense emission lines are observed for $Ba_2Eu(CO_3)_2F_3$. This feature is significant for good structural 3D order. Thus, a cationic inversion or substitution between Ba^{2+} and Eu^{3+}, eventually coupled with the substitution $CO_3^{2-} \leftrightarrow 3F^-$ for charge compensation, is excluded.

In $Eu_3(BO_3)_2F_3$, anion substitution between isoelectronic BO_3^{3-} and $3F^-$ can be assumed. The oxygen–oxygen distances in BO_3^{3-} are slightly shorter than the fluorine–fluorine distances. Consequently, deviation from the ideal stoichiometry $Eu_3(BO_3)_2F_3$ can occur, leading to the formulation $Eu_3(BO_3)_{2+x}F_{3-3x}$ with x being small. This substitution induces an evolution of the relative number of O_4F_5 and O_7F_2 polyhedra and the appearance of O_6F_3 and O_5F_4 polyhedra. Fluctuations in the crystal field of Eu^{3+} can be expected and such a disorder is compatible with the presence of broad emission lines for Eu^{3+} in $Eu_3(BO_3)_2F_3$; as mentioned heretofore, the FWHM of the emission lines is even comparable to that found in Eu^{3+}-doped glasses (6).

CONCLUSION

The crystal structure analysis indicates that similar trimeric units, $Ba_2EuO_{12}F_9$ and $Eu_3O_{14}F_9$, are found in $Ba_2Eu(CO_3)_2F_3$ and $Eu_3(BO_3)_2F_3$, respectively. There is no

TABLE 2
Crystal Field Parameters for Eu^{3+} in $Eu_3(BO_3)_2F_3$

B_q^k	Value (cm^{-1}) in C_{2v}		Value (cm^{-1}) in C_{2v}
B_0^2	−627	$N_{v,k=2}$	1089
B_2^2	−199	$N_{v,k=4}$	758
B_0^4	488	$N_{v,2+4}$	1550
B_2^4	−258	$N_{v,total}$	2040
B_4^4	−142		
B_0^6	−188		
B_2^6	−966	Nb levels	23
B_4^6	−162	σ	8.4
B_6^6	−515		

TABLE 4
Crystal Field Parameters for Eu^{3+} in $Ba_2Eu(CO_3)_2F_3$

B_q^k	Value (cm^{-1}) in C_{2v}		Value (cm^{-1}) in C_{2v}
B_0^2	264	$N_{v,k=2}$	522
B_2^2	139	$N_{v,k=4}$	894
B_0^4	−201	$N_{v,2+4}$	1343
B_2^4	−480	$N_{v,total}$	1695
B_4^4	189		
B_0^6	−217		
B_2^6	100	Nb levels	18
B_4^6	−928	σ	6.8
B_6^6	−195		

evidence of such a similarity from the optical study of Eu^{3+} luminescence. It is shown that cationic disorder between Ba^{2+} and Eu^{3+} in $Ba_2Eu(CO_3)_2F_3$ is excluded, together with the coupled substitution $CO_3^{2-} \leftrightarrow 3F^-$. In $Eu_3(BO_3)_2F_3$, the anion substitution $BO_3^{3-} \leftrightarrow 3F^-$ is probably effective and can explain the presence of broad and weak emission peaks, even for a small substitution rate. The formulation of this fluoride borate should preferably be given by $Eu_3(BO_3)_{2+x}F_{3-3x}$.

REFERENCES

1. N. Mercier and M. Leblanc, *Eur. J. Solid State Inorg. Chem.* **34,** 251 (1997).
2. T. A. Bither and H. S. Young, *J. Solid State Chem.* **10,** 302 (1974).
3. G. Corbel, R. Retoux, and M. Leblanc, *J. Solid State Chem.* **139,** 52 (1998).
4. N. Mercier and M. Leblanc, *Eur. J. Solid State Inorg. Chem.* **28,** 727 (1991).
5. G. Corbel, M. Leblanc, E. Antic-Fidancev, M. Lemaître-Blaise, and J. C. Krupa, *J. Alloys Compd.* **287,** 71 (1999).
6. G. Pucker, K. Gatterer, H. P. Fritzer, M. Bettinelli, and M. Ferrari, *Phys. Rev. B* **53,** 6225 (1996).
7. J. Hölsä, *Inorg. Chim. Acta* **139,** 257 (1987).
8. G. Chadeyron, M. El-Ghozzi, R. Mahiou, A. Arbus, and J. C. Cousseins, *J. Solid State Chem.* **128,** 261 (1997).
9. G. Chadeyron, R. Mahiou, M. El-Ghozzi, A. Arbus, D. Zambon, and J. C. Cousseins, *J. Luminescence* **72–74,** 564 (1997).
10. M. Ren, J. H. Lin, Y. Dong, L. Q. Yang, M. Z. Su, and L. P. You, *Chem. Mater.* **11,** 1576 (1999).
11. E. Antic-Fidancev, M. Lemaître-Blaise, P. Porcher, N. Mercier, and M. Leblanc, *J. Solid State Chem.* **116,** 286 (1995).
12. B. G. Wybourne, "Spectroscopic Properties of Ions in Crystals." Wiley–Interscience, New York, 1965.
13. F. Auzel and O. L. Malta, *J. Phys.* **44,** 201 (1983).